

RSC Advances



This is an *Accepted Manuscript*, which has been through the Royal Society of Chemistry peer review process and has been accepted for publication.

Accepted Manuscripts are published online shortly after acceptance, before technical editing, formatting and proof reading. Using this free service, authors can make their results available to the community, in citable form, before we publish the edited article. This *Accepted Manuscript* will be replaced by the edited, formatted and paginated article as soon as this is available.

You can find more information about *Accepted Manuscripts* in the [Information for Authors](#).

Please note that technical editing may introduce minor changes to the text and/or graphics, which may alter content. The journal's standard [Terms & Conditions](#) and the [Ethical guidelines](#) still apply. In no event shall the Royal Society of Chemistry be held responsible for any errors or omissions in this *Accepted Manuscript* or any consequences arising from the use of any information it contains.



Journal Name

ARTICLE

Broad-Spectrum Chemiluminescence Covering 400-1400 nm Spectral Region and its Use as White-Near Infrared Light Source for Imaging

Received 00th January 20xx,
Accepted 00th January 20xx

DOI: 10.1039/x0xx00000x

www.rsc.org/

Xiuping Zheng,^{ab} Wenqiang Qiao^{*a} and Zhi Yuan Wang^{*ac}

Broad-spectrum chemiluminescence (CL) from 400 nm to 1400 nm was simultaneously generated from a mixture of visible and near-infrared (NIR) fluorophores by reaction with oxalyl chloride and hydrogen peroxide. By adjusting the proportions of each of fluorophores, the white-NIR CL light could be generated and was used as a light source for tissue imaging. The samples of fresh peach leaf and a live mouse were examined under the white-NIR light using a colour camera and a NIR camera at the same time. The white-NIR CL light offered more comprehensive and in-depth information on the thin leaf tissues acquired by both colour and NIR cameras. Owing to the presence of the NIR light, this unique light source can also be used for imaging of thick animal tissues. Therefore, the white-NIR CL can be considered and employed as a universal light source for use with various imaging techniques.

Introduction

Since the “bluish-white” light or chemiluminescence (CL) was observed by Chandross from the reaction involving a peroxyoxalate generated from hydrogen peroxide, oxalyl chloride and a fluorescent dye (9,10-diphenylanthracene),¹ research on CL has focused on mechanistic study,² exploration of new fluorophores and applications. The chemiluminescent reactions involving peroxyoxalate is highly effective.^{3,4} Typically, a certain colour is generated when an oxidizing agent (hydrogen peroxide or oxygen) reacts with phthalhydrazide derivatives (e.g., luminol),^{5,6} imidazole derivatives (lophine and 2-methyl-6-(p-methoxyphenyl)-3,7-dihydroimidazo[1,2- α]pyrazin-3-one or MCLA),^{7,8,9} and acridinium derivatives.^{10,11,12} In addition, oxalyl chloride has been a common reagent in CL reactions since the work by Chandross and widely used in the visible or NIR CL systems.^{1,13,14}

Due to high sensitivity and elimination of autofluorescence interference by photoexcitation, CL is applied in ultrasensitive analysis, for example, detection of hydrogen peroxide *in vivo*¹⁵ and bioactive compounds (e.g., glucose¹⁶ and hydrogen sulfide^{17,18}), food analysis,¹⁹ organic pollutants in the environment,²⁰ and blood in forensic analysis.²¹ The CL is also widely used as a light source in imaging for biological research and physical therapy.^{22,23,24}

Compared with high energy radiation from radioisotopes, the CL imaging is particularly attractive because the chemiluminescent light is low-energy, relatively less harmless to tissues and easily detected by technically straightforward instrumentation.^{25,26,27}

At present, most CL occurs in the visible spectral region, e.g., 420–480 nm for luminol and 465 nm for MCLA in *Cypridina* luciferin analogs.^{5,28} The Burgess group demonstrated the through-bond energy-transfer cassettes based on UV-absorbing donors (luminol) and fluorescent acceptors. The cassettes of luminol-fluorescein and luminol-Nile Red emitted at 524 nm and 634 nm, respectively.²⁹ The visible CL is sensitive for the imaging of superficial or thin biological tissues, but less sensitive for thick tissues.³⁰ Due to the reduced absorption and scattering, the NIR light (700–1100 nm) has better penetration through biological tissues, which is beneficial for imaging in depth.^{31,32,33} The NIR CL has been reported in recent years. Smith and coworkers reported the interlocked fluorescent squaraine rotaxane endoperoxides, which were stable at low temperature and emitted the NIR light near 750 nm at the elevated temperatures.²⁵ Ansaldi and coworkers achieved the CL at 800 nm by the chemiluminescence resonance energy transfer from luminol-generated blue light to nanoparticles.³⁰ In addition, NIR CL tunable from 900 nm to 1700 nm was achieved using the low-bandgap compounds and polymers.¹⁴

With different tissue penetrability, both visible and NIR light are useful for bio-imaging and other imaging techniques. For example, the photosensitizers used in conventional photodynamic therapy are mostly activated by visible light to treat the tumors on or just under the skin.³³ In biometrics, the finger vein patterns could be acquired using NIR light.³⁴ Hyperspectral imaging techniques were introduced for the determination of adulteration in minced meat to overcome the disadvantages of specific wavelength measurement.³⁵ Thus, the broad-spectrum CL covering both visible

^a State Key Laboratory of Polymer Physics and Chemistry, Changchun Institute of Applied Chemistry, Chinese Academy of Sciences, Changchun 130022, P. R. China

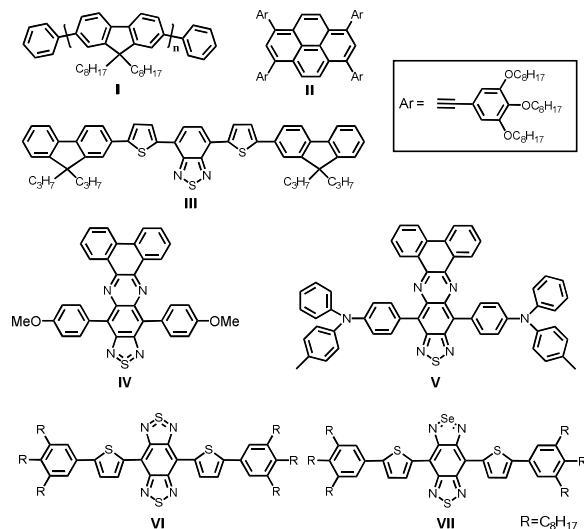
^b University of Chinese Academy of Sciences, Beijing 100049, P. R. China

^c Department of Chemistry, Carleton University, 1125 Colonel By Drive, Ottawa, Ontario, Canada K1S 5B6

† Electronic Supplementary Information (ESI) available: [Characterizations for I. Synthesis and characterizations for compounds VI and VII. Calculation of fluorescence quantum yields. The detailed procedures and the time course of the CL process. Images of peach leaf using single-fluorophore CL]. See DOI: 10.1039/x0xx00000x

and NIR spectral regions are deemed to be universal and beneficial for imaging applications. However, the currently available CL light is either colour³⁶ or NIR³⁷, rather than both or white-NIR.

Herein we present the CL covering both the visible and NIR spectral regions and its potential use as a white-NIR CL light source for tissue imaging. The white-NIR CL light was achieved using a group of fluorescent materials **I–VII** with the emission wavelengths in a range of 400–1400 nm (Chart 1). Under this broad-spectrum CL light, the animal and plant tissues were imaged concurrently with two cameras, colour (400–1000 nm) and NIR (900–1700 nm)



cameras.

Chart 1. Chemical structures of fluorophores **I–VII**.

Experimental

1. Reagents and Materials

Hydrogen peroxide (30% in water) and oxalyl chloride were obtained from commercial sources. Solvents for the emission test were purified by distillation. All the other chemicals and reagents were used as received without further purification. Polymeric fluorophore **I** and fluorescent compounds **II–V** were obtained according to the reported methods.^{38–41} Compounds **VI** and **VII** were synthesized as the routes in Scheme S1 (Supporting Information).

2. Methods

¹H (400 MHz) and ¹³C (100 MHz) NMR spectra of all the samples in chloroform were obtained using a Bruker Avance 400 NMR spectrometer. Matrix-assisted laser desorption ionization time-of-flight mass spectrometry was recorded from Bruker Daltonics Autoflex III TOF/TOF. The UV–vis–NIR absorption spectra were recorded from a Shimadzu UV-3600 spectrophotometer. The photoluminescence (PL) and chemiluminescence (CL) spectra in visible region were measured with a UV-vis fluorimeter (PE LS55).

The CL was studied with light source closed and in biolum-mode. NIR PL and CL spectra were obtained using a PTI fluorescence system with InGaAs detector. For the NIR CL measurement, the excitation source in PTI fluorescence system was turned off and the CL signal was modulated by placing a chopper between the reaction cell and the detector. The CL signals were recorded in time-base mode right after fluorescent compounds, hydrogen peroxide and oxalyl chloride were mixed together.

3. Imaging study

For imaging a plant tissue, a fresh peach leaf was picked in September in the city of Changchun, China and then was used without further treatment. The leaf thickness is about 0.5 mm.

For imaging an animal tissue, a KM mouse, aged 6–8 weeks, with a weight of 31.5 g was selected and anaesthetized using chloral hydrate through intraperitoneal injection.

For the study of maximum penetration depth by this method, thinly sliced products of fresh meat were used and measured with a vernier caliper for the thickness values.

The tissue images were captured with a colour camera (Sony NEX-5TY, silicon detector with a spectrum cut-off at 1000 nm) and a NIR camera (NIRvana camera, Princeton Instruments LightField, InGaAs detector, spectral response of 900–1700 nm).

Results and Discussion

1. Optical Property

The absorption, photoluminescence and chemiluminescence spectra of fluorophores **I–VII** were recorded in chloroform (Fig. 1). The absorption bands in the UV–vis region below 500 nm are ascribed to $\pi-\pi^*$ and $n-\pi^*$ transitions of the conjugated aromatic sections (Fig. 1a and Table 1); while the absorption bands above 500 nm are mainly owing to the charge transfer between peripheral donors and central acceptor groups. With the stronger donors or acceptors, the absorption bands shift to the lower energy regions.¹⁴ The PL spectra of **I–VII** in chloroform cover the region from 400 nm to 1400 nm (Fig. 1b and Table 1). The maximum emission wavelength is 420 nm for **I** with a quantum efficiency of 74.8%. Due to the presence of donor and acceptor groups in **III–VII**, the maximum wavelengths of the fluorescence spectra gradually shift from 636 nm to 1105 nm, along with a decrease in the emission efficiency. CL occurred when fluorophores were mixed with oxalyl chloride and hydrogen peroxide. As expected, the CL spectra (Fig. 1c) are similar to the corresponding PL spectra (Fig. 1b), which confirms the presence of the singlet-excited state of fluorophores **I–VII** as the light-emitting species.¹⁴ The slight redshift of CL maxima may be caused by reabsorption of short-wavelength emission by the fluorescent dyes in systems.⁴²

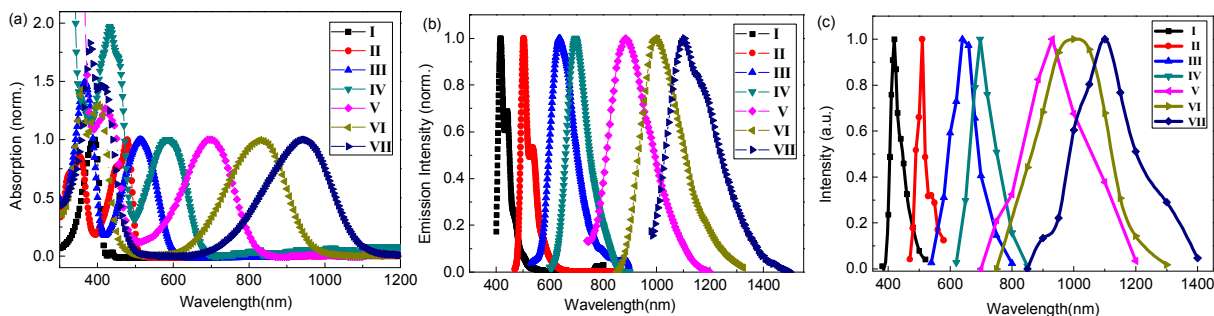


Fig. 1 (a) Absorption, (b) photoluminescence and (c) chemiluminescence spectra of I-VII in chloroform (1×10^{-5} M). For CL, hydrogen peroxide (3.93×10^{-2} M) and oxalyl chloride (3.65×10^{-2} M) were added. The PL and CL spectra of I-IV were recorded with a UV-vis fluorimeter (PE LS55) and those of V-VII were taken with a NIR fluorimeter (PTI fluorescence system). All the spectra are normalized relative to the maximal absorption or emission wavelengths.

Table 1 Absorption, photoluminescence and chemiluminescence of I-VII

	Abs λ_{\max} (nm) ^a	PL λ_{\max} (nm) ^a	ϕ_f (%) ^b	CL λ_{\max} (nm) ^c
I	392	420	74.8 ^d	420
II	478	536	60.9 ^d	540
III	514	636	49.0 ^d	645
IV	588	696	14.2 ^e	704
V	704	885	2.2 ^f	926
VI	830	995	<1 ^f	1000
VII	946	1105	<1 ^f	1100

^a Absorption and fluorescence maxima in chloroform with a concentration of 1×10^{-5} M. ^b Fluorescence quantum yield. ^c CL maximum from reaction of oxalyl chloride (3.65×10^{-2} M) and hydrogen peroxide (3.93×10^{-2} M). ^d Relative to quinine sulfate ($\phi_f = 0.55$ in 0.5 M H_2SO_4). ^e Relative to fluorescein ($\phi_f = 0.95$ in 0.1 M NaOH). ^f Relative to IR-125 ($\phi_f = 0.13$ in DMSO).

2. Time course of CL

In a typical CL reaction, hydrogen peroxide firstly reacts with oxalyl chloride to generate highly energetic dioxetanedione that excites a fluorescent compound and then the light emits.^{3,43} From the flash CL profiles (Fig. S1, Supporting Information), the CL intensity markedly increased once the CL reaction began and then decreased after very short time. Taking compound II as an example, the CL intensity at 510 nm increased to the maximum (vertical axis about 900) in 20 seconds after oxalyl chloride was injected into the system. Then, the CL intensity decreased to the minimum rapidly. The durations of the CL light and the HOMO values of the fluorophores were summarized in Table S2. Obviously, the

durations of light emission from V, VI and VII were significantly shorter than I, II, III and IV. The possible reason was that HOMO values of NIR fluorophores (V, VI and VII) were higher than the visible fluorophores (I, II, III and IV), which were considered to be more susceptible to be oxidized by dioxetanedione intermediate and therefore leading to a much faster bimolecular rate between intermediate and NIR fluorophores.

3. Effects of concentrations on chemiluminescence

There was no emission detected in absence of any of the three reactants (fluorescent compound, oxalyl chloride and hydrogen peroxide). The dependence of CL intensity on reactant concentrations was investigated by keeping the concentrations of two of the three reactants constant while varying the other one's concentration. The tests were done by monitoring CL intensity at the maximum emission wavelengths for I, III and V (Fig. 2). The CL intensity increased almost linearly with the concentration of I in a range of 10^{-6} – 10^{-5} M (Fig. 2a) and with the concentration of hydrogen peroxide being kept within a range of 7.9×10^{-4} – 2.7×10^{-3} M (Fig. 2b). In the interval of 1.8×10^{-4} – 3.7×10^{-1} M for oxalyl chloride concentration, only at a low concentration (below 1.46×10^{-2} M), the CL intensity had a nonlinear increase (Fig. 2c). However, at a higher concentration of oxalyl chloride, a large amount of hydrochloric acid was generated, thus inhibiting the formation of dioxetanedione and hindering the further CL process.

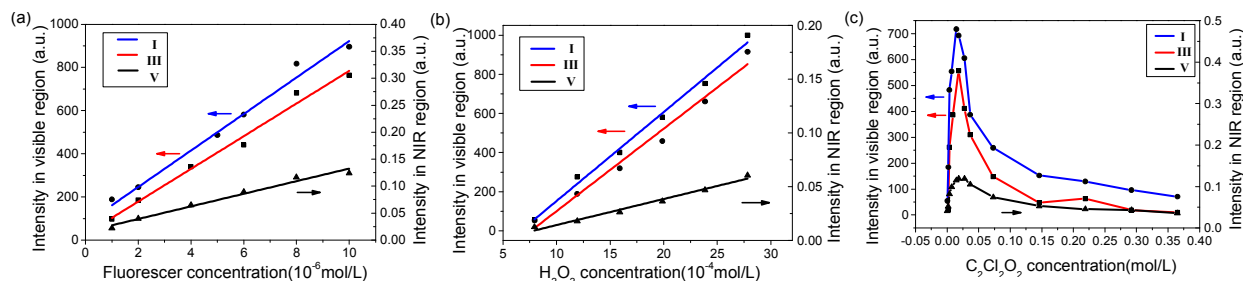


Fig. 2 Studies of the effect of the reactant concentrations on the CL process. (a) Changes in fluorophore concentration; constant concentrations of hydrogen peroxide (3.93×10^{-2} M) and oxalyl chloride (3.65×10^{-2} M). (b) Changes in hydrogen peroxide concentration; constant concentrations of fluorophores (1×10^{-4} M) and oxalyl chloride (1.83×10^{-2} M). (c) Changes in the oxalyl chloride concentration; constant concentrations of fluorophores (1×10^{-4} M) and hydrogen peroxide (1.96×10^{-3} M). The CL from fluorophores I and III were recorded with a UV-vis fluorimeter (PE LS55) and those from fluorophore V were recorded with the NIR fluorimeter (PTI fluorescence system).

4. CL spectra

4.1 CL spectra of single-fluorophore and multi-fluorophores

Under the optimized concentrations of hydrogen peroxide and oxalyl chloride, the CL spectra from a single fluorophore to multi-fluorophores were recorded (Fig. 3). Fig. 3a shows the CL spectrum of fluorophore I in chloroform (1×10^{-5} M) and the inset illustrates the photos of its solution taken before (left) and after (right) being treated with oxalyl chloride and hydrogen peroxide. The CL with a maximum at 420 nm is consistent with the PL maximum emission wavelength. To broaden the CL spectral range, fluorophores II–IV were individually introduced into the CL systems. Fig. 3b displays

the CL spectrum of the mixture of fluorophores I and II with a molar ratio of 10/1. Clearly, the CL spectral range expanded from 420 nm to 550 nm and the colour of CL light became green (Figure 3b). With the three (I–III) and four (I–IV) fluorophores, the CL spectra extended to 700–800 nm and the systems emitted the white light (Fig. 3c and 3d). Similarly, a mixture of NIR fluorophores V, VI and VII (molar ratio 1/1/2) gave the broad CL spectrum from 800 nm to 1400 nm (Fig. 3e). The invisible CL light was captured using the NIR camera (inset, Fig. 3e).

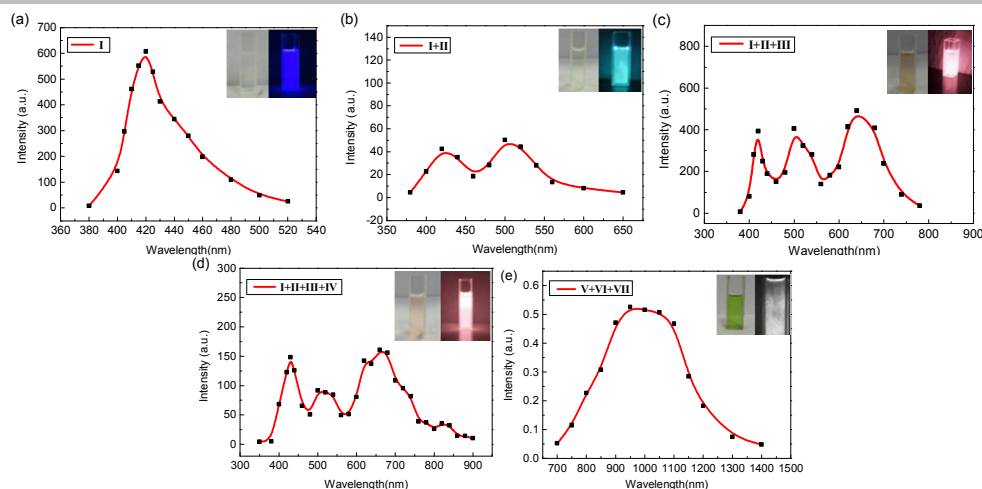


Fig. 3 CL spectra of single-fluorophore (a) and multi-fluorophores (b–e) containing hydrogen peroxide (3.93×10^{-2} M) and oxalyl chloride (1.46×10^{-2} M). Insets are the photos taken before (left) and after (right) the addition of oxalyl chloride. The photos on the right (inset in a–d) were taken with a colour camera and the right one in (e) was taken with a NIR camera.

4.2 White-NIR CL

Accordingly, by blending the visible and NIR fluorophores I–VII in certain proportions, the broad-spectrum CL from 400 nm to 1400 nm was achieved (Fig. 4). The image *a* (inset in Fig. 4) shows the original colour of the mixture of I–VII in chloroform observed by the naked eyes (or a colour camera). When CL occurred, the colour appeared to be white as observed with a colour camera (image *b* in Fig. 4), and the NIR CL light (image *c* in Fig. 4) was revealed using a NIR camera.

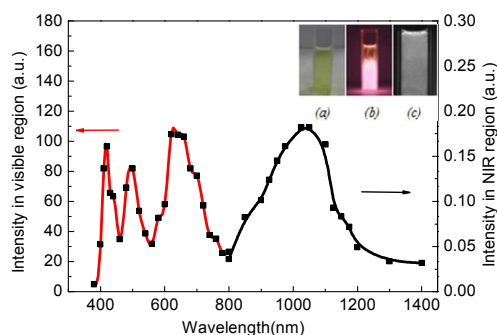


Fig. 4 White-NIR CL spectra generated from a mixture of I–VII. Concentrations: I (1.97×10^{-6} M), II (3.94×10^{-7} M), III (9.85×10^{-7} M), IV (3.94×10^{-6} M), V (7.39×10^{-6} M), VI (2.61×10^{-6} M), VII (1.48×10^{-5} M), hydrogen peroxide (3.93×10^{-2} M) and oxalyl chloride (1.46×10^{-2} M). Inset: photos (*a*) and (*b*) taken with a colour camera before and after addition of oxalyl chloride; photo *c* taken with a NIR camera.

5. Energy transfer in CL systems

Considering the energy transfer (ET) between fluorescent compounds during the CL process, molar ratios of these fluorophores were adjusted to achieve broad-spectrum CL. For example, the molar ratio of I/II was adjusted to 10/1 in order to obtain the similar CL intensity at the respective maximum emission wavelengths (420 nm for I and 500 nm for II, Fig. 3b). Because the fluorescent molecules in solution could diffuse freely and intermolecular collisions were expected to take place, the non-radiative ET in the CL process was mainly governed by the Dexter exchange mechanism.⁴⁴ The main factors of influencing the energy transfer efficiency are spectral overlap, the relative orientation of the transition dipoles and relative distance between the host (energy donor) and guest (energy acceptor).^{45,46} Spectral overlaps between the normalized host emission and guest absorption (Fig. 1

and Table 1) indicated that a fairly easy energy transfer between fluorescent compounds could occur in the system. Under the same conditions (e.g., solvent, concentration and temperature), the probability of fluorescent molecules being excited by the energetic dioxetanedione intermediate was different because of the distinct oxidation potentials (according to the HOMO in Table S2) and steric effects of fluorophores, resulting in unequal reaction rate between the intermediate and fluorophores. Due to the very short duration time of CL (Fig. S1) and long intermolecular distances in diluted solutions, energy transfer between fluorescent compounds occurred partially but not completely. So the higher energy could not be completely quenched but weakened to a certain extent. Therefore, only by adjusting the proportion of fluorescent molecules, could the CL with nearly equal intensity over a wide spectral region be achieved.

6. Imaging Application

CL imaging *in vitro* under this white-NIR light source for biological tissues has been explored. Two independent studies were carried out with a leaf and a live mouse as samples.

6.1 Leaf imaging

The detailed experimental setup for CL imaging of fresh leaf was depicted in Fig. 5a. The CL light from a small groove containing a solution of fluorophores, hydrogen peroxide and oxalyl chloride passed through the leaf (positioned on the transparent plate) between the groove and the camera. Under the daylight without CL, the leaf appeared to be normal green colour with main veins on surface (Fig. 5b). In dark, under the white-NIR CL light, more structural details and fine veins were revealed with a colour camera (Fig. 5c). Meanwhile, being observed by a NIR camera, main veins in leaf became translucent, as a result of the NIR light penetrating through the veins (Fig. 5d).

Furthermore, leaf imaging under the single-fluorophore CL light was carried out for comparison (Fig. S2). Leaf veins under green light from II (Fig. S2c) had better definition compared with blue light from I and red light from III or IV (Fig. S2b and Fig. S2d), which were mainly attributed to less absorption of green light by leaf cells. However, none of them gave a better image than that obtained under the white-NIR CL light. In the NIR region, the results from single-fluorophore V, VI and VII were basically identical and similar to the white-NIR light (Fig. S2e). Therefore, in comparison with daylight or single-fluorophore CL, the white-NIR CL light offered more comprehensive and in-depth information on the leaf tissues acquired by both colour and NIR cameras.

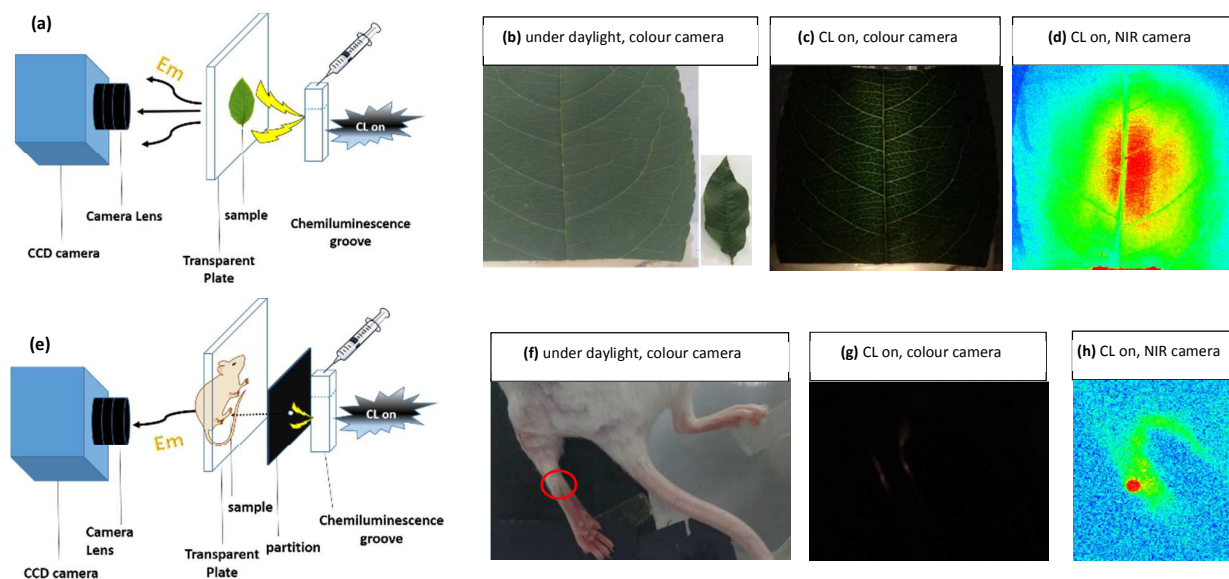


Fig. 5 Imaging studies of a leaf and a live mouse: Experimental set-up for the leaf (a) and mouse (e) imaging; Photographs of the leaf (b) and the live mouse (f) taken with a colour camera under daylight; Photographs of the leaf (c) and the live mouse (g) taken with a colour camera under white-NIR CL light; Photographs of the leaf (d) and the live mouse (h) taken by a NIR camera under white-NIR CL light. The location to be observed on the mouse leg was marked by the red circle (f). Hydrogen peroxide (3.93×10^{-2} M), oxalyl chloride (1.46×10^{-2} M), the concentrations of the fluorophores I-VII were ten times as those for the white-NIR CL spectrum in Fig. 4.

6.2 Mouse imaging

The CL imaging of a live mouse was studied. The experimental operation was similar to that for the leaf imaging except for the use of a black baffle to allow a beam of light to pass through (Fig. 5e). The mouse was anaesthetized and put on the transparent plate 10 minutes later. Fig. 5f shows the photograph of the mouse in bright-field and the imaging position at the rear leg (4.2 mm) is marked by a red circle. Under the white-NIR CL light, the images were obtained with a colour camera and as well NIR camera. As shown in Fig. 5g, with a colour camera the image was dark and unsatisfactory because no white light could be expected to pass through the thick tissues. Similarly, for imaging under the colour CL light from I, II, III or IV, no signal was detected by the colour camera because of very low penetration of colour light through thick tissues.

In contrast, with a NIR camera, the bright region at the mouse leg was observed under the white-NIR CL light (Fig. 5h) or under the NIR light from single-fluorophore V, VI and VII. Thus for thick tissues imaging, it is necessary to use the NIR light regardless of the image diffusion due to planar optical imaging.⁴⁷ Furthermore, the maximum penetration depth by this method was studied using several thicknesses of fresh meat tissues and the depth was

approximately 1.87cm (Fig.S3, Supporting Information). Therefore, this white-NIR CL light can be very useful for the imaging of thick animal tissues.

Conclusions

The broad-spectrum CL from 400 nm to 1400 nm has been readily accessible by selecting a group of visible-NIR fluorescent materials. The CL spectral profiles were adjusted simply by changing the proportion of each of fluorophores, in order to realize the white-NIR CL. As demonstrated, thin plant tissues (fresh leaf) or thick animal tissues (live mouse) could be examined by direct imaging under the white-NIR CL light concurrently with a colour camera and NIR camera. Accordingly, the white-NIR CL can be considered and employed as a universal light source for use with various imaging techniques. Comprehensive information of the tissues with different thicknesses can be acquired simultaneously by examination with two cameras (colour camera and NIR camera), thus avoiding replacement of the single-fluorophore CL source, simplifying the experimental process and improving the reliability of the imaging results at the same time.

Acknowledgements

This work was supported by National Natural Science Foundation of China (21134005, 21474102 and 21474105) and the Natural Science and Engineering Research Council of Canada.

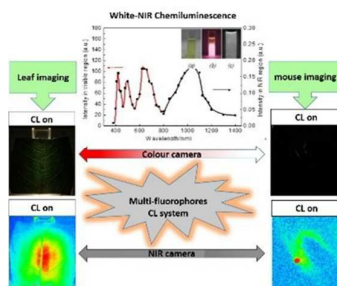
References

- 1 E. A. Chandross, *Tetrahedron Lett.*, 1963, **4**, 761-765.
- 2 C. V. Stevani, S. M. Silva and W. J. Baader, *Eur. J. Org. Chem.*, 2000, **2000**, 4037-4046.
- 3 L. F. M. L. Ciscato, F. H. Bartoloni, E. L. Bastos and W. J. Baader, *J. Org. Chem.*, 2009, **74**, 8974-8979.
- 4 M.A. de Oliveira, F. H. Bartoloni, F. A. Augusto, L. F. M. L. Ciscato, E. L. Bastos and W. J. Baader, *J. Org. Chem.*, 2012, **77**, 10537-10544.
- 5 E. H. White and M. M. Bursley, *J. Am. Chem. Soc.*, 1964, **86**, 941-942.
- 6 A. Roda, M. Guardigli, E. Michelini, M. Mirasoli and P. Pasini, *Anal. Chem.*, 2003, **75**, 462A-470A.
- 7 E. H. White and M. J. C. Harding, *J. Am. Chem. Soc.*, 1964, **86**, 5686-5687.
- 8 K. Sugioka, M. Nakano, S. Kurashige, Y. Akuzawa and T. Goto, *FEBS Lett.*, 1986, **197**, 27-30.
- 9 Y. Tampo, M. Tsukamoto and M. Yonaha, *FEBS Lett.*, 1998, **430**, 348-352.
- 10 C. Lee and L. A. Singer, *J. Am. Chem. Soc.*, 1980, **102**, 3823-3829.
- 11 M. M. Rauhut, D. Sheehan, R. A. Clarke, B. G. Roberts and A. M. Semsel, *J. Org. Chem.*, 1965, **30**, 3587-3592.
- 12 (a) F. McCapra, *J. Chem. Soc., Chem. Commun.*, 1977, 946-948. (b) M. Mitani, Y. Koinuma, K. Fugami and M. Kosugi, *Polym. J.*, 1996, **28**, 671-677.
- 13 P. Lovera, K. Reynolds and G. Redmond, *Phys. Status Solidi A*, 2009, **206**, 2240-2244.
- 14 G. Qian, J. P. Gao and Z. Y. Wang, *Chem. Commun.*, 2012, **48**, 6426-6428.
- 15 C.-K. Lim, Y.-D. Lee, J. Na, J. M. Oh, S. Her, K. Kim, K. Choi, S. Kim and I. C. Kwon, *Adv. Funct. Mater.*, 2010, **20**, 2644-2648.
- 16 P. Panoutsou and A. Economou, *Talanta*, 2005, **67**, 603-609.
- 17 T. S. Bailey and M. D. Pluth, *J. Am. Chem. Soc.*, 2013, **135**, 16697-16704.
- 18 J. Cao, R. Lopez, J. M. Thacker, J. Y. Moon, C. Jiang, S. N. S. Morris, J. H. Bauer, P. Tao, R. P. Mason and A. R. Lippert, *Chem. Sci.*, 2015, **6**, 1979-1985.
- 19 S. Bezzi, S. Loupassaki, C. Petrakis, P. Kefalas and A. Calokerinos, *Talanta*, 2008, **77**, 642-646.
- 20 Y. Hu and Z. Yang, *Talanta*, 2004, **63**, 521-526.
- 21 F. Barni, S. W. Lewis, A. Berti, G. M. Miskelly and G. Lago, *Talanta*, 2007, **72**, 896-913.
- 22 Y. Zhang, L. Pang, C. Ma, Q. Tu, R. Zhang, E. Saeed, A. E. Mahmoud and J. Wang, *Anal. Chem.*, 2014, **86**, 3092-3099.
- 23 T.-C. Chena, L. Huang, C.-C. Liua, P.-J. Chao, F.-H. Lin, *Process Biochem.*, 2012, **47**, 1903-1908.
- 24 F. Bonvicini, M. Mirasoli, G. Gallinella, M. Zerbini, M. Musiania and A. Roda, *Analyst*, 2007, **132**, 519-523.
- 25 J. M. Baumes, J. J. Gassensmith, J. Giblin, J.-J. Lee, A. G. White, W. J. Culligan, W. M. Leevy, M. Kuno and B. D. Smith, *Nat. Chem.*, 2010, **2**, 1025-1030.
- 26 J. G. Mancini and M. N. Ferrandino, *Curr. Opin. Urol.*, 2010, **20**, 163-168.
- 27 J. R. Bading, M. Hörling, L. E. Williams, D. Colcher, A. Raubitschek and S. E. Strand, *Cancer Biother Radio*, 2008, **23**, 399-410.
- 28 K. Teranishi, *Luminescence*, 2007; **22**, 147-156.
- 29 J. Han, J. Jose, E. Mei and K. Burgess, *Angew. Chem. Int. Ed.*, 2007, **46**, 1684-1687.
- 30 N. Zhang; K. P. Francis; A. Prakash and D. Ansaldi, *Nat. Med.*, 2013, **19**, 500-505.
- 31 G. Lapadula, D. Trummer, M. P. Conley, M. Steinmann, Y.-F. Ran, S. Brasselet, Y. Guyot, O. Maury, S. Decurtins, S.-X. Liu, and C. Copereț, *Chem. Mater.*, 2015, **27**, 2033-2039.
- 32 N. Ma, A. F. Marshall and J. Rao, *J. Am. Chem. Soc.*, 2010, **132**, 6884-6885.
- 33 N. M. Idris, M. K. Gnanasammandhan, J. Zhang, P. C. Ho, R. Mahendran and Y. Zhang, *Nat. Med.*, 2012, **18**, 1580-1585.
- 34 E. C. Lee, H. Jung, and D. Kim, *Sensors*, 2011, **11**, 2319-2333.
- 35 M. Kamruzzaman, Y. Makino, S. Oshita and S. Liu, *Food Bioprocess Technol*, 2015, **8**, 1054-1062.
- 36 Y.-D. Lee, C.-K. Lim, A. Singh, J. Koh, J. Kim, I. C. Kwon and S. Kim, *ACS nano*, 2012, **6**, 6759-6766.
- 37 J.-J. Lee, A. G. White, D. R. Rice and B. D. Smith, *Chem. Commun.*, 2013, **49**, 3016-3018.
- 38 J. Liu, Q. Zhou, Y. Cheng, Y. Geng, L. Wang, D. Ma, X. Jing and F. Wang, *Adv. Funct. Mater.*, 2006, **16**, 957-965.
- 39 A. Hayer, V. de Halleux, A. Köhler, A. El-Garouhy, E. W. Meijer, J. Barberá, J. Tant, J. Levin, M. Lehmann, J. Gierschner, J. Cornil and Y. H. Geerts, *J. Phys. Chem. B*, 2006, **110**, 7653-7659.
- 40 G. Qian, X. Li and Z. Y. Wang, *J. Mater. Chem.*, 2009, **19**, 522-530.
- 41 G. Qian, Z. Zhong, M. Luo, D. Yu, Z. Zhang, D. Ma and Z. Y. Wang, *J. Phys. Chem. C*, 2009, **113**, 1589-1595.
- 42 M. M. Rauhut, B. G. Roberts, D. R. Maulding, W. Bergmark and R. Coleman, *J. Org. Chem.*, 1975, **40**, 330-335.
- 43 D.-Q. Yuan, N. Kishikawa, C. Yang, K. Koga, N. Kuroda and K. Fujita, *Chem. Commun.*, 2003, 416-417.
- 44 N. J. Turro, *Modern Molecular Photochemistry*, The Benjamin Cummings Publishing Co. Inc., Menlo Park, CA, 1978, Ch. 9.
- 45 J.-L. Brédas, D. Beljonne, V. Coropceanu and J. Cornil, *Chem. Rev.*, 2004, **104**, 4971-5004.
- 46 S. Bag, J.-C. Tseng and J. Rochford, *Org. Biomol. Chem.*, 2015, **13**, 1763-1767
- 47 Tuchin, V. V. *Tissue Optics* 2nd edn (SPIE Press, 2007).

Journal Name

ARTICLE

Table of Contents



Broad-spectrum chemiluminescence has been achieved and used as a white-near infrared light source for imaging techniques.